Structural Engineering and Mechanics, *Vol. 72, No. 3 (2019) 395-408*
DOI: https://doi.org/10.12989/sem.2019.72.3.395

Seismic response of RC frames under far-field mainshock and near-fault aftershock sequences

Seyed Amin Hosseini[1a], Jorge Ruiz-García[2b] and Ali Massumi*[1]

[1]*Department of Civil Engineering, Faculty of Engineering, Kharazmi University, Tehran, Iran*
[2] *Department of Civil Engineering, Universidad Michoacana de San Nicolás de Hidalgo, Mexico City, Mexico*

(Received September 3, 2018, Revised April 22, 2019, Accepted July 2, 2019)

Abstract. Engineered structures built in seismic-prone areas are affected by aftershocks in addition to mainshocks. Although aftershocks generally are lower in magnitude than that of the mainshocks, some aftershocks may have higher intensities; thus, structures should be able to withstand the effect of strong aftershocks as well. This seismic scenario arises for far-field mainshock along with near-field aftershocks. In this study, four 2D reinforced concrete (RC) frames with different numbers of stories were designed in accordance with the current Iranian seismic design code. As a way to evaluate the seismic response of the case-study RC frames, the inter-story drift ratio (IDR) demand, the residual inter-story drift ratio (RIDR) demand, the Park-Ang damage index, and the period elongation ratio can be useful engineering demand parameters for evaluating their seismic performance under mainshock-aftershock sequences. The frame models were analyzed under a set of far-field mainshock, near-fault aftershocks seismic sequences using nonlinear dynamic time-history analysis to investigate the relationship among IDR, RIDR, Park-Ang damage index and period ratio experienced by the frames. The results indicate that the growth of IDR, RIDR, Park-Ang damage index, and period ratio in high-rise and short structures under near-fault aftershocks were significant. It is evident that engineers should consider the effects of near-fault aftershocks on damaged frames that experience far-field mainshocks as well.

Keywords: mainshock-aftershock sequences; inter-story drift ratio; residual inter-story drift ratio, damage index, period elongation, reinforced concrete frames

1. Introduction

Man-made structures located in earthquake-prone regions are not exposed to a single seismic event, but also to a seismic sequence consisting of foreshocks, the mainshock and aftershocks. According to Bath's law, the average difference in magnitude between a mainshock and its largest aftershock is very stable (typically 1.2), regardless of the mainshock magnitude (Shcherbakov *et al.* 2005). For this reason, it is usually expected that the peak ground acceleration, PGA, of the mainshock recorded in an accelerographic station should be greater than that of the largest aftershock. However, an unusual seismic scenario could occur when the PGA of the mainshock is smaller than the PGA of the aftershock. This situation arises when the recording station at a given site is located at a shorter epicentral distance from the aftershock epicenter than that from the mainshock epicenter. That is, structures could experience a far-field and a near-fault earthquake ground motion during a seismic sequence. For instance, this unusual seismic scenario occurred during the strong seismic events that struck the Southern Island of New Zealand when a strong mainshock occurred on September 3, 2010 (M_w = 7.0) in the Canterbury region followed by several strong aftershocks, on February 21, 2011 (M_w = 6.3) that severely hit the city of Christchurch. As a consequence, several recording stations located near the Christchurch recorded greater PGAs due to the aftershock than those from the mainshock (e.g. Bradley 2012). Particularly, the 2011 aftershock event caused 185 fatalities and severe structural damage, or even collapse, in many commercial, residential, and industrial structures (Potter *et al.* 2015). However, seismic design codes worldwide still use a single "design earthquake" for design purposes and they do not take into account the effects of the aftershocks in calculating the inelastic response of structures (ACI 318-08, Eurocode 8 2005, Iranian code, Standard 2800, 2005).

The main objective of this paper is to examine the seismic response of a family of reinforced concrete (RC) frames under a far-field (FF) mainshock and near-fault (NF) aftershock (FF-NF) scenario. For this purpose, typical RC frames designed with the Iranian Code were subjected to a relatively large set of artificial seismic sequences to investigate the relationship of maximum (peak) inter-story drift and residual (permanent) inter-story drift with respect to the well-known Park-Ang damage index (Park and Ang 1985, Park and Ang 1985).

2. Brief literature review

Several studies on the performance of engineered structures, particularly RC frames, subjected to mainshock-aftershock seismic sequences have been carried out up to date. These research studies have been developed using

*Corresponding author, Professor
E-mail: massumi@khu.ac.ir
[a] MS, graduated
E-mail: s.amin9068@gmail.com
[b] Professor
E-mail: jruizgar@stanfordalumni.org

http://www.techno-press.com/journals/sem&subpage=7
ISSN: 1225-4568 (Print), 1598-6217 (Online)

single-degree-of-freedom (SDOF) or multi-degree-of-freedom (MDOF) systems. Early studies to evaluate the inelastic response demand of structures induced by seismic sequences were carried out from inelastic single-degree-of-freedom (SDOF) systems. For instance, Mahin (1980) investigated the non-linear response of SDOF systems under mainshock-aftershock earthquake ground motions recorded during the 1972 Managua earthquakes. The author observed that the displacement ductility demand and the energy dissipation demand of elastoplastic SDOF systems slightly increased as a consequence of the aftershock. Years later, Hatzigeorgiou and Beskos (2009) studied the effects of successive earthquakes on the inelastic displacement ratio of SDOF systems, and they proposed a new equation for estimating the inelastic displacement ratio under mainshock-aftershock sequences. Zhai *et al*. (2013, 2014) investigated structural damage in SDOF systems subjected to mainshock-aftershocks events. They first presented a simplified method for simulation of a mainshock-aftershock sequence based on a modified form of Bath's law, while evaluated the damage spectra under several acceleration time histories representing a mainshock along aftershocks with larger peak ground acceleration, or two relatively moderate aftershocks. They found that the aftershocks had a significant effect on the structural damage of SDOF systems. Multiple relatively moderate aftershocks had a noticeable effect on structural damage in comparison with the effect of the largest aftershock. Zhai *et al*. (2014) focused their attention on the structural damage of SDOF systems under mainshocks which were followed by aftershocks having different relative peak ground accelerations (PGAs). It confirmed that the effect of a weak aftershock can be ignored in the evaluation of damage of SDOF systems; however, moderate and strong aftershocks have significant effects on such systems. Ductility-based strength reduction factor, $R\mu$, for mainshock-aftershock consecutive ground motions was proposed by Zhai *et al*. (2015). To assess this parameter, they used 458 multiple seismic sequences and four hysteresis structural models. The results revealed that the effect of multiple strong aftershocks on $R\mu$ is greater in the short period region than a region with a long period. More recently, Yaghmaei-Sabegh and Ruiz-García (2016) presented a case study on the nonlinear response of SDOF systems subjected to mainshock-aftershock sequences recorded during the 2012 Varzaghan-Ahar earthquakes occurred in the Northwestern zone of Iran. Their study was done in two parts. The first part studied the frequency content characteristics of the Varzaghan-Ahar seismic sequences. The results showed that the seismic energy for the individual sequences with respect to multiple earthquakes could be significant. The second part compared the formula suggested by another researcher when evaluating $R\mu$ and the inelastic displacement ratio (IDR) under multiple events. The results indicated that the predictions have been underestimated for intermediate- and long-period spectral regions. Zhang *et al*. (2017) investigated damage-based strength reduction factor for multiple ground motions. They considered SDOF systems with 30 periods which endured five levels of ductility and five damage index levels under 342 mainshock and 342 mainshock-aftershock ground motions. The results revealed that the strength reduction factors were strongly affected by the aftershock events.

Additionally, several studies have investigated the effects of aftershocks on multiple-degree-of-freedom (MDOF) structures. For instance, Bazzurro *et al*. (2004) proposed guidelines for the seismic evaluation of buildings under aftershocks that take into account the loss in strength capacity of a building previously damaged under the mainshock. They prepared a tagging methodology to assess the consideration of aftershock hazard and acceptable risk levels after the effect of the mainshock. Years later, Ruiz-García and Negrete-Manriquez (2011) assessed the inelastic response of multi-story steel frames subjected to near-fault (NF) and far-field (FF) mainshock-aftershock sequences recorded during Californian earthquakes (e.g., the 1994 Northridge and 1980 Mammoth Lakes earthquakes). The results showed that aftershocks having a predominant period close to the period of vibration of the frame significantly increased the peak and residual drift demand of the case-study steel frames. Faisal *et al*. (2013) investigated the story ductility demand of reinforced concrete frames with 3, 6, 12, and 18 stories under multiple earthquakes. They considered three mainshock-aftershocks pairs which included single, double and triple shocks. The results showed that multiple earthquakes created a dramatic growth in the story ductility of concrete buildings. Ruiz-García *et al*. (2014) investigated the effects of multiple earthquakes on reinforced concrete structures located in soft-soil sites. They analyzed four frames having different numbers of stories that were subjected to artificial sequences simulated from the events in Mexico City on the September 19 and the September 20, 1985 earthquakes. The results revealed that the nonlinear response of frames is strongly related to the ratio of the dominant period of the aftershock to the dominant period of the mainshock. They reported that aftershocks having dominant period close to the predominant period of vibration of the damaged frames were strongly significant. A parametric investigation on the effect of mainshock-aftershock events on the seismic response of RC frames was performed by Abdelnaby and Elnashai (2015). The results showed that the effects of repeated earthquakes on the RC frames was significant and that the seismic performance of a damaged frame under multiple earthquakes decreases dramatically. Moustafa and Takewaki (2012) studied the different parameters of mainshock-aftershock sequences and the effects of these kinds of multiple events on the damage accumulation and the inelastic response of structures. Ruiz-García and Aguilar (2015) proposed a methodology for seismic evaluation of aftershocks that considers residual drift, which appears in a damaged structure after the mainshock. They used four mainshock-aftershock scenarios that are likely to occur in a seismic area. It should be noted that this methodology was initially proposed for a 4-story case-study frame. The results revealed that one of most effective aspects of achieving a realistic inelastic response of a frame, such as the collapse potential, relates to the modeling approach. They specified that the aftershock collapse capacity was greater than that associated with the residual inter-story drift that causes impending collapse.

Maniyar *et al*. (2009) studied seismic performance of existing RC frames by considering the yielding and collapse capacity of the frames. They generated a method of predicting probability of yielding and collapse which depends upon earthquake intensity. Kim and Kim (2007) assessed the seismic performance of RC frames by designing a frame based on the 2003 IBC code and investigating the seismic responses of the frame under several inelastic time history analyses. They modified the FEMA-355F process for assessment of the seismic performance of RC frames and suggested that overestimation of the seismic safety of buildings has emerged because of the use of deterministic analysis results for demand and capacity.

Considering the initial damage pattern and spectral shape, a study on aftershock collapse fragility was performed by Liu, Yu *et al*. (2018). Results showed that the collapse capacity of damaged frame is directly related to the initial damages and it would decrease as initial damage raise. Moreover, a linier correlation model was suggested between the collapse capacity and aftershock spectral shape.

Mirtaheri *et al*. (2017) conducted a research on residual displacement of low to medium rise steel frames equipped with cylindrical frictional damper under aftershock effects. The results showed that residual drifts enhance as the result of second shock.

A risk-based evaluation of seismic performance of RC frame subjected to multiple earthquakes was studied by Shokrabadi and Burton (2018). It was found that considering the risk of aftershocks over the risk of mainshock could result in an increase around three times in the collapse of structures during their usual lifetime (50 years). Then, they suggested that seismic risk of aftershocks should be considered during the structural design process.

Hosseinpour and Abdelnaby (2017) studied the effects of i) damage from mainshock, ii) mainshock-aftershock direction, iii) the third (vertical) component of sequences, and iv) aftershock polarity. They found that the first three items have a significant effect on seismic performance under mainshock-aftershock sequences. Furthermore, under the influence of aftershocks, irregular buildings underwent massive seismic responses.

Naderpour and Vakili (2019) investigated the seismic performance of shear wall-frame RC structures by developing fragility and vulnerability curves under mainshock-after shock sequences. The study results showed that the structures have weak seismic performances under the influences of mainshock-aftershock sequences.

Diaz-Martinez, *et al*. (2014) studied the impacts of narrow-banded seismic sequences on two steel-moment resisting frames that house essential facilities were designed according to the 2004 edition of the Mexico City Building Code. They found that seismic response of frame depends on fundamental periods of vibration of frame and dominant period of the mainshock.

Kostinakis and Morfidis (2017) studied the effects of mainshock-aftershock events on damage level of 3D reinforced concrete structures, with different load bearing systems. The results showed that damage level of structures experienced a remarkable rise under effect of seismic sequences comparing to the effect a single event.

Lateral strength and damage of reinforcement concrete frames, which have different between design considerations and construction (known as deviation) was investigated by Massumi *et al*. (2018). The results showed that deviation in strength of reinforcements is more important than concrete strength.

Kang and Lee (2016) developed a new structural damage index for RC columns based on a local tensile damage variable. This new damage index is useful for seismic fragility analysis and can use for prediction of the local damages of RC columns.

Sakka *et al*. (2018) suggested a reliability-based methodology for evaluating damaged RC members and purposed a reliability index that is used to assess structural component of damaged frames.

Habibi *et al*. (2018) studied on assessment of seismic performance of RC frames with different setbacks under earthquake events. They found that the element which is located close to setback experienced a severe damage under seismic shocks.

Recently, several investigations have proposed new approaches for revision of the damage index, which can be useful for the seismic evaluation of structures under seismic sequences. For instance, Cao *et al*. (2014) collected all useful and available damage indices which considered both local and global damage. They proposed a new energy damage index based on both static and cyclic performance. Chen and Xu (2007) proposed a new damage index which considers quick stiffness degradation during earthquakes. Moustafa and Takewaki (2010) suggested a new approach to simulation of near-fault earthquakes which depends on the structural damage index, energy rate and frequency content.

A new method for damage evaluation of RC frames based on the relationship between period elongation and the Park-Ang damage index was presented by Massumi and Moshtagh (2013). Recently, Aghagholizadeh and Massumi (2016) developed that mentioned damage index. They presented a new damage index which depends on higher modes. The results show that period elongation could be a useful and reliable dynamic parameter to represent the damage state of a frame after an earthquake. Significant growth in period elongation was recorded after the severe damage state.

In the current study, the critical scenario of a mainshock-aftershock event is presented and the IDR, RIDR, damage index and period of the damaged frames was investigated.

3. Building frame models and ground motions

3.1 Case-Study building frame models and modeling approach

In this investigation, four regular three-bay RC buildings having 4, 8, 12, and 16 stories were designed in accordance to the Iranian seismic design code (Standard 2800, 2005). The buildings were designed with a typical story-height and width of 3 m and 5 m, respectively. Nominal yield stress of steel reinforcement and the compressive stress of the concrete were assumed as 390 MPa and 24.5 MPa, respectively, in the design process. The plan and elevation view of the frames is shown in Fig. 1 and the geometry and element sections of the frames are reported in Table 1. For analysis purposes, a frame representative of each building was modeled as bi-dimensional centerline model using the nonlinear dynamic analysis computer program IDARC2D (Reinhorn *et al.* 2009). Beams and columns were modeled as frame elements which concentrate their inelastic response in plastic hinges located at their ends. In IDARC2D (Reinhorn *et al.* 2009), the hysteretic behavior in the plastic hinges is modeled through the three-parameter model, which requires the definition of four parameters to define the level of unloading stiffness degradation, cyclic strength-degradation and pinching. In this study, it was assumed that the RC beams and columns exhibits slight stiffness degradation (HC = 10), moderate strength-degradation (HBD = 0.30, HBE = 0.15), and negligible pinching (HS = 1.0). Further details of the design and modeling of the case-study RC frames can be found in Hosseini (2016).

Before performing nonlinear dynamic analysis, ordinary modal analysis and nonlinear static (pushover) analysis were carried out to obtain main dynamic and mechanical properties of the four frame models. Table 2 reports the first-mode period of vibration, T1, yield drift ratio, Θ_y, and the yield strength coefficient, C_y, while Fig. 2 shows a comparison of the capacity curves (i.e., base shear normalized with respect to the frame's weight, V_b/W, versus roof drift ratio) obtained for all frames.

3.2 Mainshock-Aftershock seismic sequences

Different mainshock-aftershock sequence-type events can be identified in a seismic sequence: (i) far field mainshock-far field aftershock (FF-FF sequence), (ii) near fault mainshock -near fault aftershock (NF-NF sequence), (iii) far field mainshock -near fault aftershock (FF-NF sequence), and (iv) near fault mainshock -far field aftershock (NF-FF sequence). It should be noted that in all types of sequences, the mainshock have larger magnitude than their aftershocks, but in scenarios such as the FF-NF sequence, the NF aftershocks can have a larger peak ground acceleration than their corresponding FF mainshock. This situation can be explained since the stations can be located at a shorter epicentral distance from the aftershock epicenter than that from the mainshock epicenter. This could be a consequence of what seismologists call "aftershock migration", which means that the rupture of asperities and barriers in a fault triggers aftershocks. Aki (1984) found they are strong patches of the fault plane that are resistive to breaking, which explains the irregular slip motion over a heterogeneous fault plane. That is, an asperity/barrier release the stress concentration caused by the mainshock in the surrounding area and, as a consequence, it triggers the aftershock. In fact, larger asperity areas are related to large earthquakes (Ruff and Kanamori 1983).

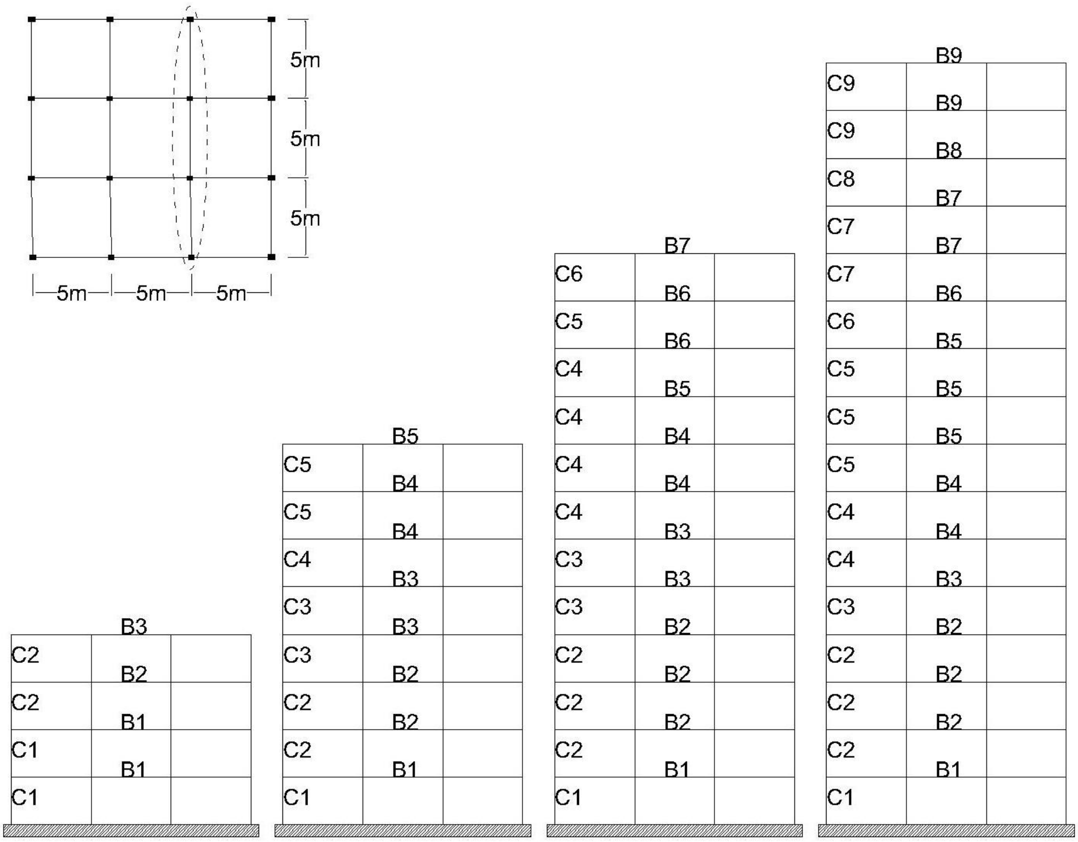

Fig. 1 Plan view and elevation of the case-study RC frames

Table 1 Details of RC elements in the case-study frames

Frame	Column section	Dimension (width×depth) (mm)	Reinforcement steel area (mm^2)	Beam section	Dimension (width×depth) (mm)	Reinforcement steel area (mm^2)	
						Bottom	Top
4 story	C1	450×450	2713.0	B1	450×400	763.0	1526.0
	C2	400×400	2713.0	B2	400×400	763.0	1526.0
				B3	400×400	508.7	1017.4
8 story	C1	550×550	5024.0	B1	550×500	1271.0	2034.7
	C2	500×500	5024.0	B2	500×450	1780.0	2543.4
	C3	450×450	5024.0	B3	450×400	1526.0	2543.4
	C4	400×400	4069.4	B4	400×400	1017.4	1780.0
	C5	400×400	2411.6	B5	400×400	508.7	1017.4
12 story	C1	600×600	6079.0	B1	600×550	1526.0	2034.7
	C2	550×550	6079.0	B2	550×500	1780.0	2798.0
	C3	500×500	6079.0	B3	500×450	2034.7	2798.0
	C4	450×450	4069.4	B4	500×450	2034.7	2798.0
	C5	400×400	4069.4	B5	450×400	1526.0	2798.0
	C6	400×400	2411.6	B6	400×400	1017.0	2798.0
				B7	400×400	763.0	1017.0
16 story	C1	700×700	6079.0	B1	700×650	1526.0	2034.7
	C2	650×650	6079.0	B2	650×650	1780.0	2798.0
	C3	600×600	6079.0	B3	600×550	2289.1	3306,0
	C4	550×550	6079.0	B4	550×500	2289.1	3306.0
	C5	500×500	6079.0	B5	500×450	2289.1	2798.0
	C6	500×500	5023.0	B6	500×450	1526.0	2289.1
	C7	450×450	4069.4	B7	450×400	1526.0	2289.1
	C8	450×450	2411.4	B8	450×400	763.0	1017.0
	C9	400×400	2411.4	B9	400×400	763.0	1017.0

Table 2 Dynamic and mechanical properties of the case-study frame models

Frame model	T_1 (s)	Θ_y (%)	C_y
4-story	0.69	0.47	0.22
8-story	1.10	0.46	0.18
12-story	1.40	0.39	0.15
16-story	1.66	0.38	0.12

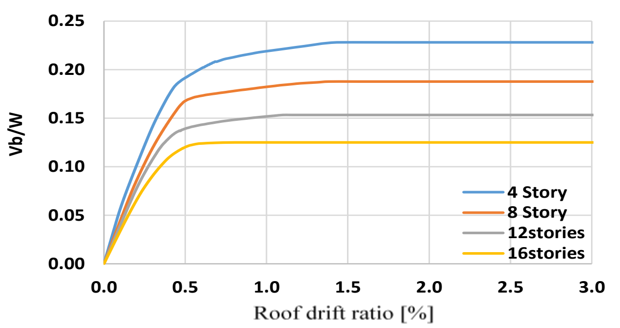

Fig. 2 Comparison of capacity curves, Vb/W vs. roof drift ratio, of the case-study RC frames

Therefore, "aftershock migration" can lead to the seismic scenario where the epicenter of the aftershock is closer than the epicenter of the mainshock, which was observed in the 2010–2011 New Zealand earthquakes (Bradley, 2012). Another unusual seismic sequence scenario arises when two mainshocks separated in time and location trigger earthquake recordings is an accelerographic stations, which are called "doublet earthquakes", such as the 2012 Varzaghan–Ahar earthquakes (e.g., Yaghmaei-Sabegh and Ruiz-García, 2016). To illustrate the effects of these four seismic sequence scenarios, a comparison of the inter-story drift ratio time-histories for the upper story of the 8-story frame is shown in Fig. 3. It is clear that the FF-NF scenario is the most critical among other four sequences since the building model exhibits small permanent displacement after the FF mainshock, although it significantly increases the drift response under a severe NF aftershock even more than 2-fold compared to the peak drift and permanent drift triggered by the mainshock. Moreover, it is believed that the quantity of earthquake effects directly depends on both natural frequency models and existing frequency content.

For performing nonlinear dynamic time-history analysis of the case-study frames, 10 as-recorded (real) mainshock-

Table 3 Ground motions recorded during the September 3, 2010 and February 21, 2011 Canterbury earthquakes

Station ID	Station name	Date (MODYYR)	Comp.	D* [km]	PGA [m/s^2]	T_m** [s]	Shock type
SHLC	Shirley Library	030910	S40W	39.0	1.71	0.76	FF-Mainshock
		022211	S40W	9.0	3.06	0.95	NF-Aftershock
		030910	S20E	39.0	1.76	1.06	FF-Mainshock
		022211	S50E	9.0	3.35	1.03	NF-Aftershock
CCCC	Christchurch Cathedral College	030910	N64E	38.0	2.25	0.98	FF-Mainshock
		022211	N64E	6.0	4.74	1.18	NF-Aftershock
		030910	N26W	38.0	1.99	1.38	FF-Mainshock
		022211	N26W	6.0	3.60	1.16	NF-Aftershock
CBGS	Christchurch Botanic Gardens	030910	N89W	36.0	1.47	0.80	FF-Mainshock
		022211	N89W	9.0	5.19	1.05	NF-Aftershock
		030910	S01W	36.0	1.71	1.30	FF-Mainshock
		022211	S01W	9.0	4.22	0.79	NF-Aftershock
CHHC	Christchurch Hospital	030910	N01W	36.0	1.94	1.78	FF-Mainshock
		022211	N01W	8.0	3.30	0.94	NF-Aftershock
		030910	S89W	36.0	1.49	0.94	FF-Mainshock
		022211	S89W	8.0	3.54	1.14	NF-Aftershock
CMHS	Christchurch Cashmere High School	030910	N10E	36.0	2.33	0.82	FF-Mainshock
		022211	N10E	6.0	3.89	0.82	NF-Aftershock
		030910	S80E	36.0	2.44	0.48	FF-Mainshock
		022211	S80E	6.0	3.48	0.79	NF-Aftershock

*epicentral distance; **mean period

aftershock sequences gathered during the September 3, 2010 (Mw = 7.0) earthquake and the strong aftershock occurred on February 21, 2011 (Mw = 6.1) in the Canterbury region of New Zealand were selected for this investigation. Table 3 reports relevant ground motion features of the selected earthquake ground motions. These seismic sequences are representative of a FF-NF sequence scenario (Ruiz-García, 2013), which means that some stations recorded greater peak ground acceleration due to the aftershock than those from the mainshock. For illustration purposes, Fig. 4 (left side) shows a FF-NF seismic sequence recorded at Christchurch Cashmere High School Station (N10E component) from the 2010/2011 New Zealand earthquakes, where it is evident the differences in amplitude, frequency content, and duration. The right-hand side of the Fig. 4 shows the acceleration response spectra computed from the individual records and the sequence. It can be seen that the acceleration response spectra of the mainshock-aftershock sequence coincide with the acceleration response spectra of the aftershock, which means that the aftershock event dominates the response although it is an event of smaller magnitude than the mainshock.

Since ten seismic sequences are a small sample, artificial FF-NF seismic sequences were generated in this investigation. For this purpose, the “back-to-back” and the “randomized” approach has been commonly employed in previous studies (Ruiz-García, 2012). The first approach consists on repeating the real mainshock, at scaled or identical amplitude, as an artificial aftershock, which assumes that the ground motion features such as frequency content and strong motion duration of the mainshock and the aftershock is the same. The second approach consists on ensemble a set of as-recorded mainshocks, and generating artificial sequences by selecting a mainshock and simulating the remaining aftershocks by repeating the mainshock wave format repeatedly, at reduced or identical amplitude, with no change in spectral content as an artificial aftershock. Therefore, this study employed the randomized approach to generate additional 90 artificial mainshock-aftershock sequences from the mainshock and aftershock earthquake ground motions listed in Table 3. That is, an artificial sequence was assembled by selecting a mainshock from one station and adding the aftershock recorded at another station, so that a total of 90 mainshock-aftershock sequences in addition of the 10 as-recorded mainshock-aftershock sequences were used for carrying out nonlinear dynamic time-history analyses. The aftershocks were scaled to a similar peak ground acceleration equal to 0.35g, which implies that the mainshocks were also scaled in a proportional manner with respect to the aftershocks.

It should be mentioned that there is a time-gap of 200 seconds of zero-acceleration ordinates between the mainshock and the aftershock acceleration time histories to ensure that the frame reaches its steady-state position. For illustration purposes, Fig. 5 shows the roof displacement time-history of the 8-story frame under a typical FF-NF sequence recorded at Christchurch Cashmere High School Station (N10E component), where it can be seen that the NF aftershock significantly increase the roof displacement of

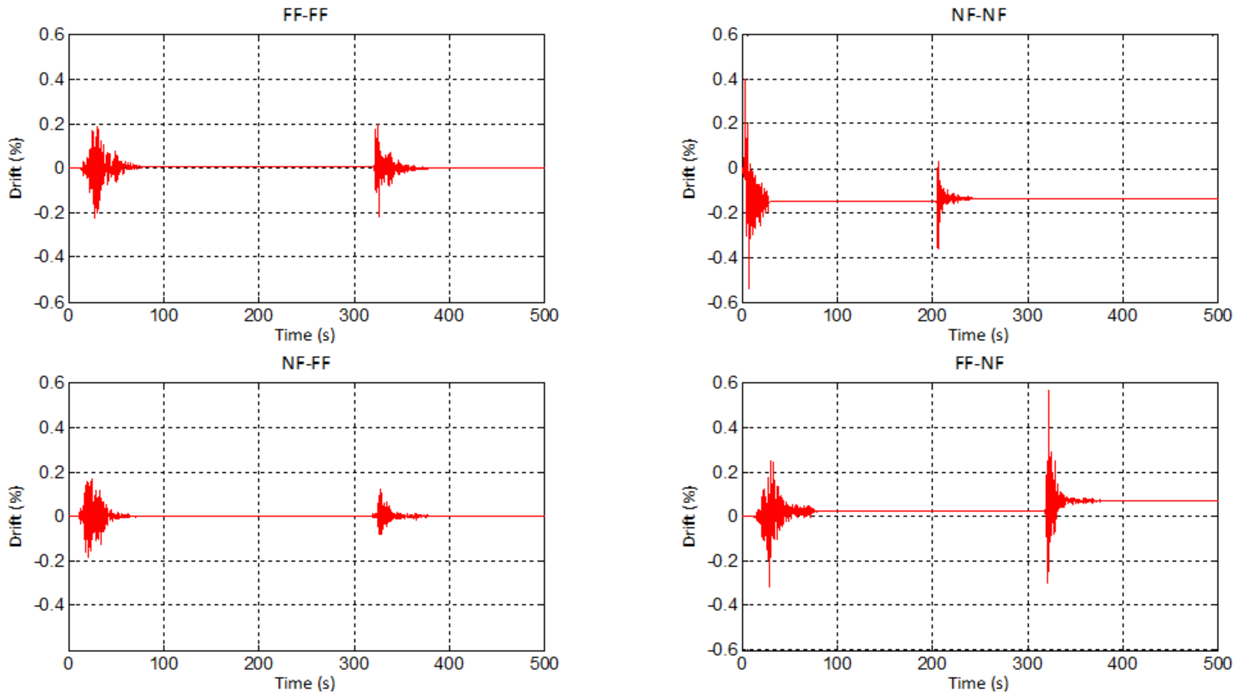

Fig. 3 Comparison of the roof drift time-history of the 8-story frame model under four mainchok-aftershock scenarios

this frame. A map from IDARC2D (Reinhorn, 2009) describing the state of damage of the 8-story frame after the mainshock and the aftershock is shown in Fig. 6a. It is interesting to note that plastic hinges appeared after the FF mainshock and NF aftershock as shown in Fig. 6 (left). Although the mainshock caused plastic hinges and cracking in the beams, additional plastic hinging in some columns and local failure in some beams occurred in the damaged frame after the effect of the NF aftershock. Fig. 6 (right) shows the base shear versus roof displacement from the dynamic time-history analysis of the 8-story frame, where it can be seen the significant difference in global hysteretic behavior.

4. Response of RC frames under mainshock-aftershock seismic sequences

In order to study the influence of FF-NF seismic sequences in the seismic response of the case-study RC frames, a series of nonlinear time-history dynamic analyses were carried out for each frame model when subjected to all sequences. The individual results were statistically processed to obtain the central tendency of peak (transient) inter-story drift demand (i.e., relative inter-story displacement normalized with respect to the story height), IDR, residual inter-story drift demand (i.e., relative permanent inter-story displacement at the end of the earthquake excitation normalized with respect to the story height), RIDR, and the damage index under the effect of the FF-NF sequences.

4.1 IDR and RIDR Demand

The effect of the mainshock-aftershock sequences on the IDR and residual inter-story demand of structures were investigated using the average (i.e., sample mean) inter-story drift ratio, AVR.IDR, and the average residual inter-story drift ratio, AVR.RIDR, demand for each frame model. To provide a context of the results, the relationship between IDR and damage levels for moment-resisting RC frames introduced by Ghobarah (2004) was taken into account in this investigation and it is reported in Table 4.

Figs. 7-8 show the height-wise distribution of AVR.IDR and AVR.RIDR for each frame under all FF-NF sequence scenarios. Particularly, Fig. 7 reveals that the AVR.IDR of all frames under the FF-NF events significantly increases with respect to those computed only under the mainshock. For example, the AVG.IDR values for the 4^{th}, 7^{th}, 3^{rd}, and 4^{th} floor of the 4-, 8-, 12-, and 16-story frames, respectively, increased more than 7-, 5-, 4-, and 6-fold compared to the effects of the mainshock alone on the frames. Moreover, it is evident that the frame models subjected to the mainshock generally experienced repairable damage (D1), but the effect of the aftershocks trigger severe damage to the RC frames. In fact, aftershocks led to the imminent collapse of the top three stories of the 4- and 8-story frames, while this situation also occurs at the 3^{rd}, 4^{th}, and 5^{th} floors of the 12-story frame. It is evident that FF mainshock did not cause the collapse of RC frames, but that strong NF aftershocks caused severe damage, or even collapse. Generally, collapse occurred in the top and bottom stories of the 4-, 8-, 12- and 16-story frames.

In addition, Fig. 8 shows the height-wise distribution of the AVR.RIDR demand for all frames in general, similarly to the previous observations for AVR.IDR, a significant increment in AVR.RIDR was caused by the strong NF aftershocks following the FF mainshocks, which only cause a slight damage to the frame models. For example, the AVG.RIDR for the 3rd, 7th, 4th, and 4th floors of the 4-, 8-,

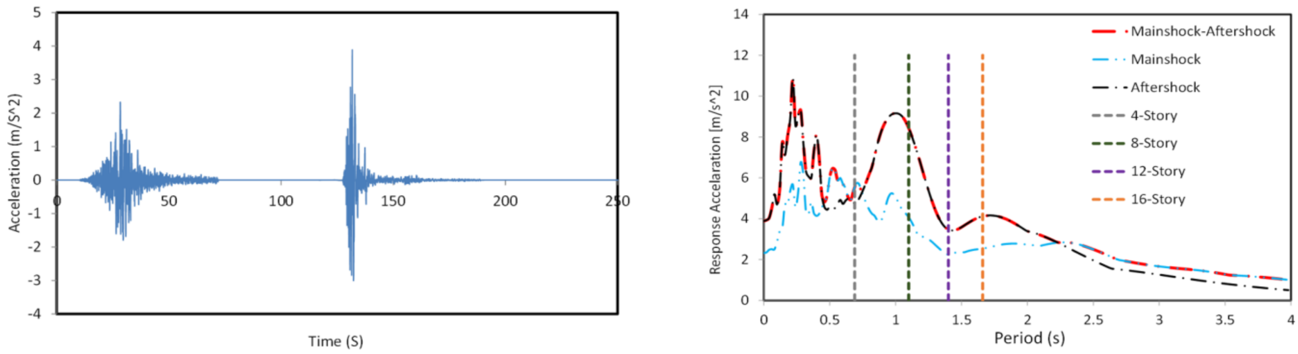

(a) Seismic sequence recorded (b) Acceleration response spectra

Fig. 4 Seismic sequence recorded at Christchurch Cashmere High School Station (N10E component), and acceleration response spectra (right-hand side), which include the fundamental periods of vibration of the case-study frames

Table 4 IDR limits for different damage levels (Ghobarah, 2004)

State of damage	IDR (%)
No damage (D0)	<0.2
Repairable damage (D1)	<1.0
Irreparable damage (D2)	<1.8
Severe damage (D3)	<3.0
Collapse (D4)	>3.0

12- and 16-story frames increased more than 12-, 8-, 4-, and 6-fold over the effects of the mainshock alone. In the medium-height frames, the AVR.IDR and AVR.RIDR demand is evident in the top and bottom stories, however, for the highest and the shortest frames, these parameters appeared in the bottom and top stories, respectively.

In summary, the NF aftershocks strongly effected both AVR.IDR and AVR.RIDR of the frames. The increment in both demand parameters is more evident in the top floors of the 4- and 8-story frames, while this situation occurs in the bottom floors of the 12- and 16-story frames. The height-wise distribution of AVG.IDR and AVG.RIDR demands for the tall buildings can be explained due to P-Δ effects. Finally, Fig. 9 shows the relationship between IDR and RIDR under the effect of FF mainshock-NF aftershock sequences. As it can be seen, the relationship between IDR and RIDR for frames which endured light and moderate damage is not as close as in cases with severe damage. The R^2 parameter shows an acceptable correlation between IDR and RIDR.

4.2 Damage index

Several damage indexes have been proposed in the literature for numerically quantifying structural damage. In this investigation, the well-known Park–Ang damage index (Park *et al.* 1985a, 1985b) was used to quantify the structural damage in the RC frames subjected to FF mainshock -NF aftershock sequences. It should be mentioned that the Park-Ang damage index was calibrated with the structural damage observed in RC buildings, and Table 5 reports the calibrated Park-Ang damage index, DI, associated to a state of damage and repairability.

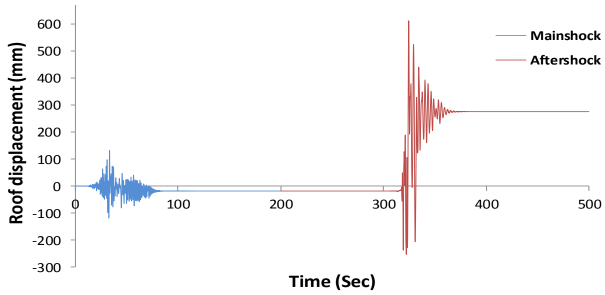

Fig. 5 Roof displacement history of 8-story frame under a typical FF-NF sequence recorded at Christchurch Cashmere High School Station (N10E component)

In the few studies who have examined the effect of seismic sequences using the DI, most researchers have examined the response of SDOF frames and a few of them MDOF systems. The research focusing on the damage index generally used one frame and artificial records for time history analysis. The current study aimed to discover a relationship among IDR, RIDR, and the DI, which help to describe the trend of growth between these parameters as affected by FF mainshock-NF aftershock sequences.

Figs. 10-11 show the evolution of DI versus the IDR and RIDR values of frames under the effects of a FF mainshock-NF aftershock sequences. As it can be seen, an increment in DI is related to the increment in IDR and RIDR of all frames affected by aftershocks. Particularly, the increment in DI follows a linear trend with respect to IDR once the frames are hit by the mainshock and they are subjected to the NF aftershocks (red triangle marks). From the Figures and values of Table 5, it can be observed that all frames experienced slight to minor damage under mainshock events, which also means a repairable damage state. Additionally, it is evident that the NF aftershocks increase the post-mainshock state of damage to reach the severe damage state. However, it can also be seen that the DI evolution is different for the case-study frames, which can be related to the particular evolution of AVG.IDR shown in Fig. 7. For instance, the 4-story building differed exhibited larger AVG.IDR in the top stories, while larger AVG.IDR was observed on the bottom stories of the 16-story frame. Similar behavior can be observed for the relationship between DI and RIDR as shown in Fig. 11.

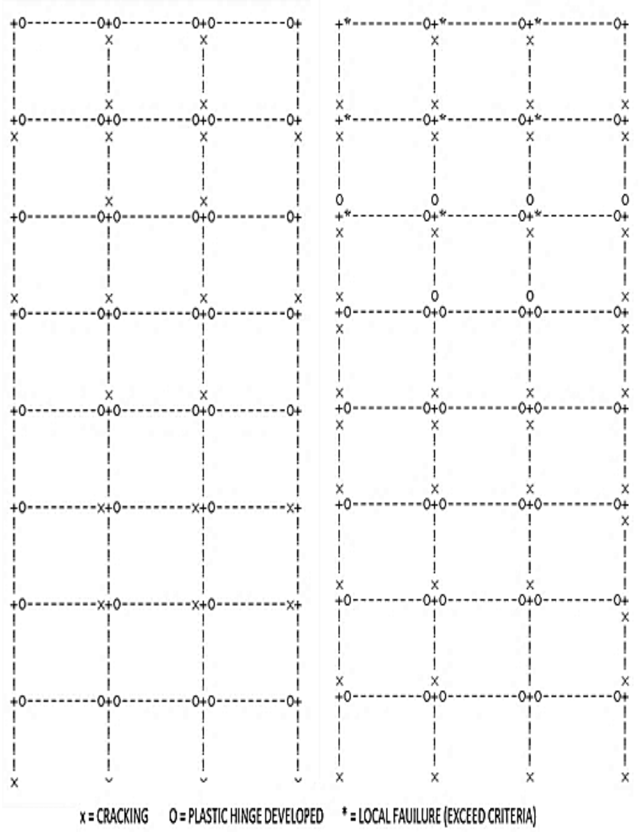

(a) Damaged frame after the mainshock (left) and the aftershock (right)

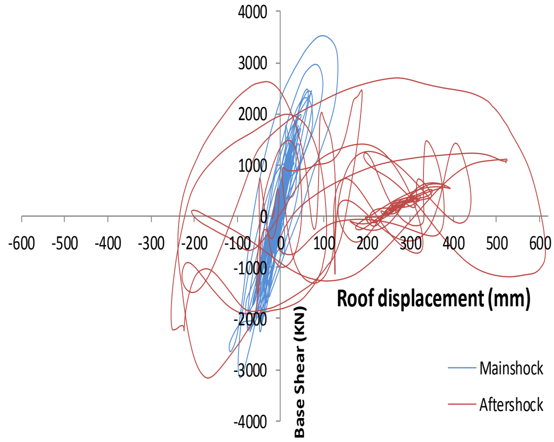

(b) Comparison of base shear vs. roof displacement

Fig. 6 The 8-story frame under a FF-NF sequence scenario

Table 5 Park-Ang damage index (Park *et al.* 1985)

State of damage	State of repairability	DI
Slight damage	Repairable damage	<0.10
Minor damage	Repairable damage	<0.25
Moderate damage	Repairable damage	<0.40
Severe damage	Irreparable damage	<1.00
Collapse	Irreparable damage	>1.00

These trends can be described mathematically as Eq. (1)

$$DI = aIDR + b \tag{1}$$

where *DI* is the Park-Ang damage index (Park *et al.* 1985a, 1985b), *a* is the gradient and *b* is the DI intercept. In summary, Table 6 reports the *a* and *b* parameters for all frames. It should be mentioned that all frames experienced damage under the effects of the FF mainshocks, associated to parameter *b*, while the level of damage increased significantly after the mainshock.

An examination of Table 6 reveals that parameter *a* seems to increase as the number of stories increases, which means that the DI is larger for the 12- and 16-story frames than for the 4- and 8-story frames for the same level of IDR or RIDR. This situation may arise due to the inter-story drift concentration in the bottom stories of the taller frames and, in consequence, to the damage accumulation due to P-effects.

Fig. 12 shows the relationship between DI versus the period ratio under the selected seismic sequences. The period ratio was computed as the period of vibration of a damaged frame after an aftershock, TD, over the period of vibration assuming elastic behavior of the frame, TE (i.e., TD/TE). To calculate the period of vibration of a damaged frame, the software IDARC (Reinhorn *et al.* 2009) stores the stiffness matrix and the mass matrix at a certain time and then calculate their dynamic properties. Thus, after the effect of each shock, the period of damaged frame is recalculated based on the updated matrices. It should be noted that the mass matrix is fixed whereas the stiffness matrix changed, since the evolution of structural degradations in the RC elements. From the Figure, it is clear that as the number of stories increased, the slope of the trend line increased. The increment in the period of the 4-story damaged frame shows a stronger trend than that of the other frames.

From this study, it should be noted that RC frames that sustain slight and moderate damage under FF mainshocks will likely sustain significant damage, and even collapse, after a strong NF aftershock. As the number of stories increases, the damage to the frames migrates from the top to the bottom stories. This migration is more critical for tall buildings. Therefore, a structural designer should consider the effect of strong aftershocks on the top and bottom stories for short and tall structures, respectively.

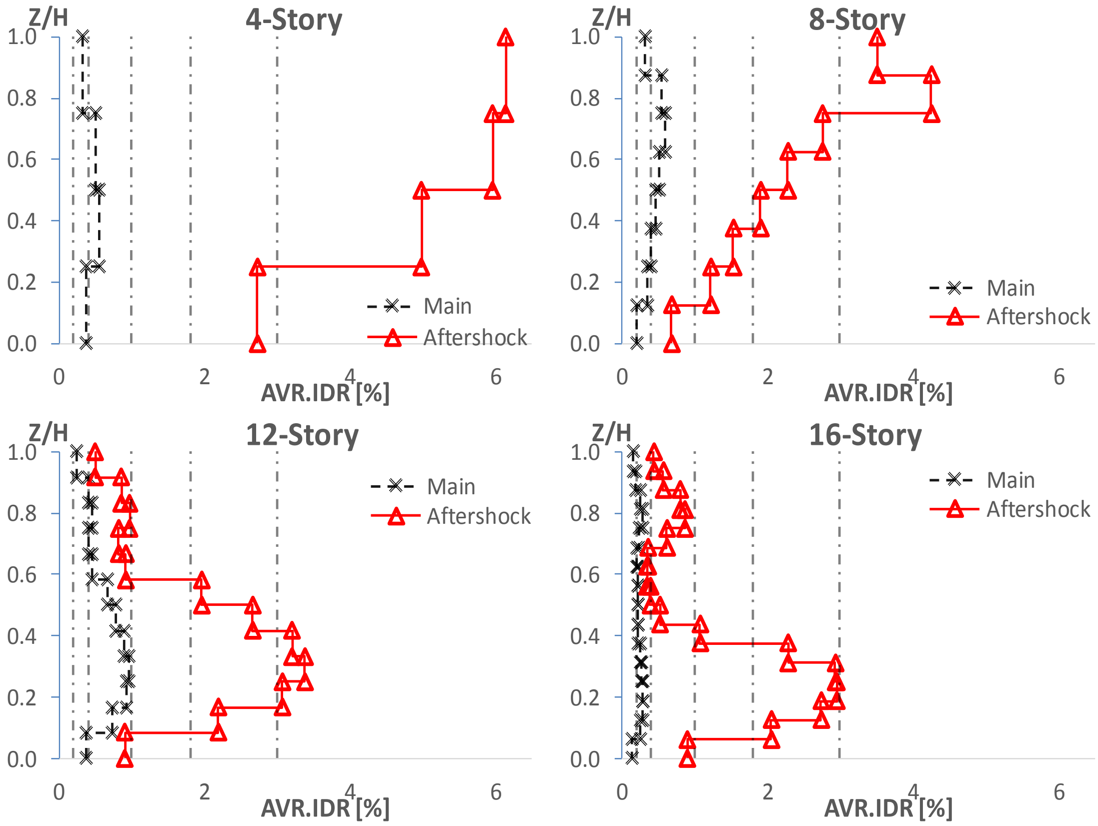

Fig. 7 Height-wise distribution of AVG.IDR demand for all frames

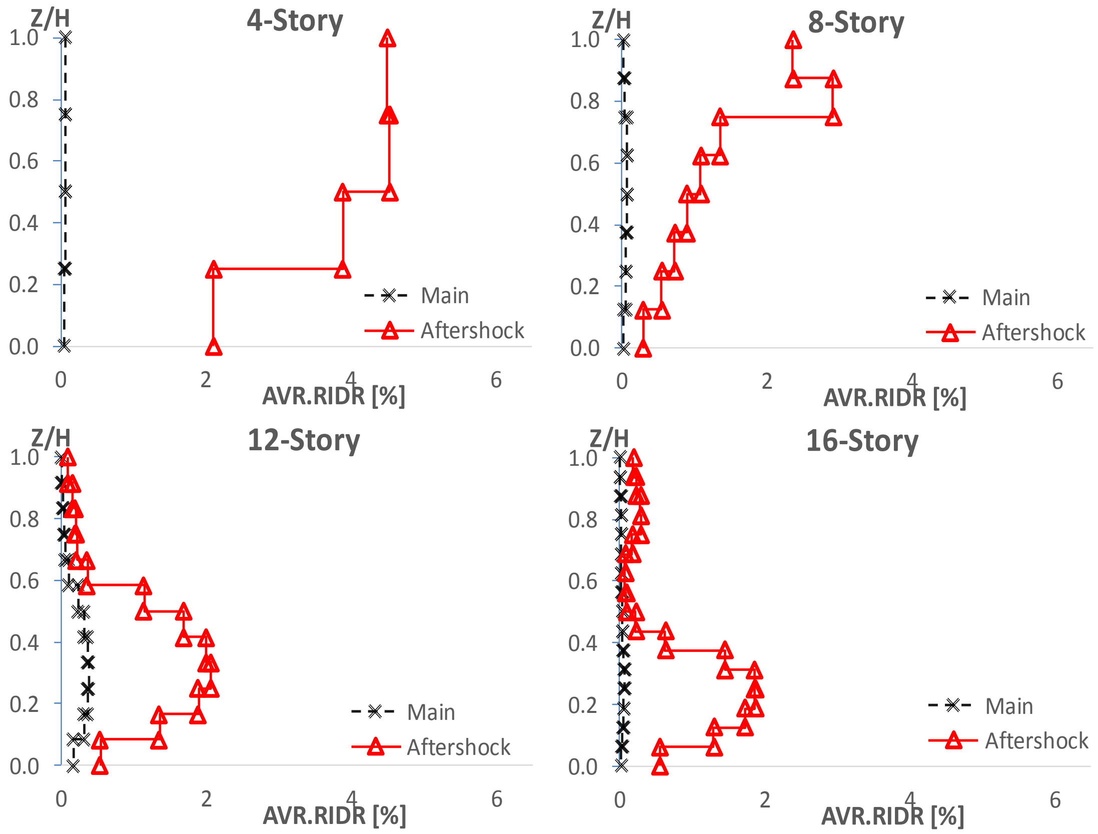

Fig. 8 Height-wise distribution of AVG. RIDR demands for all frames

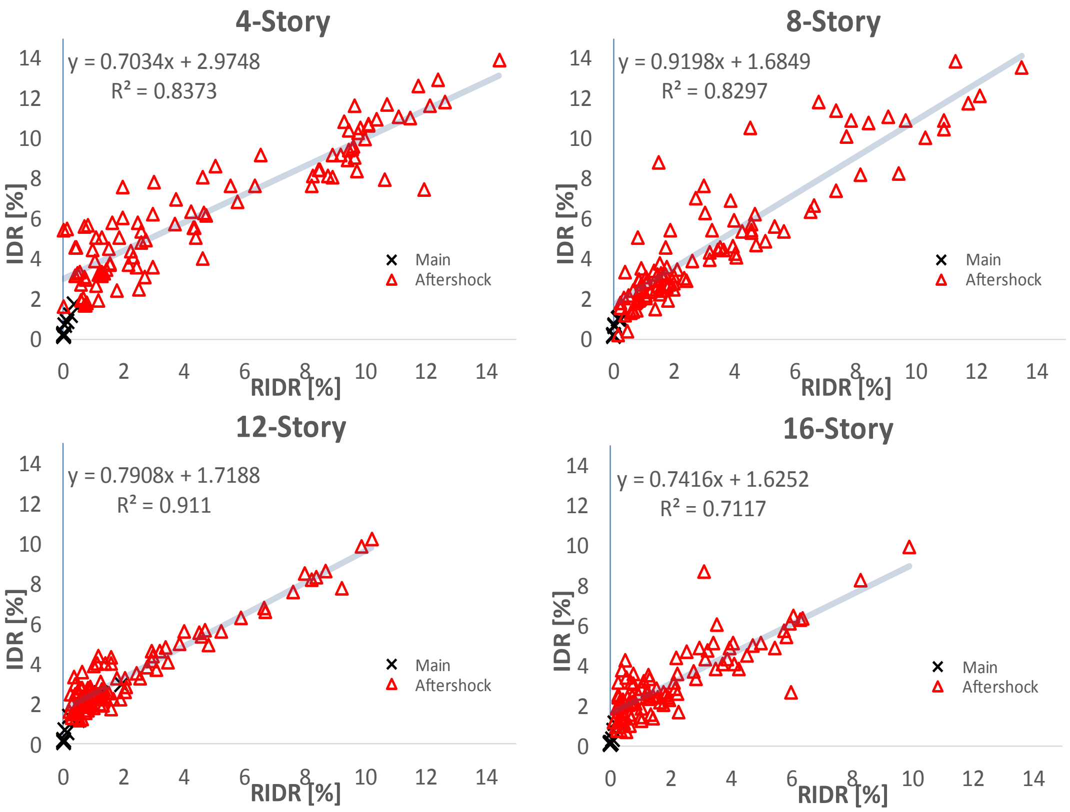

Fig. 9 IDR vs RIDR during FF-NF sequences

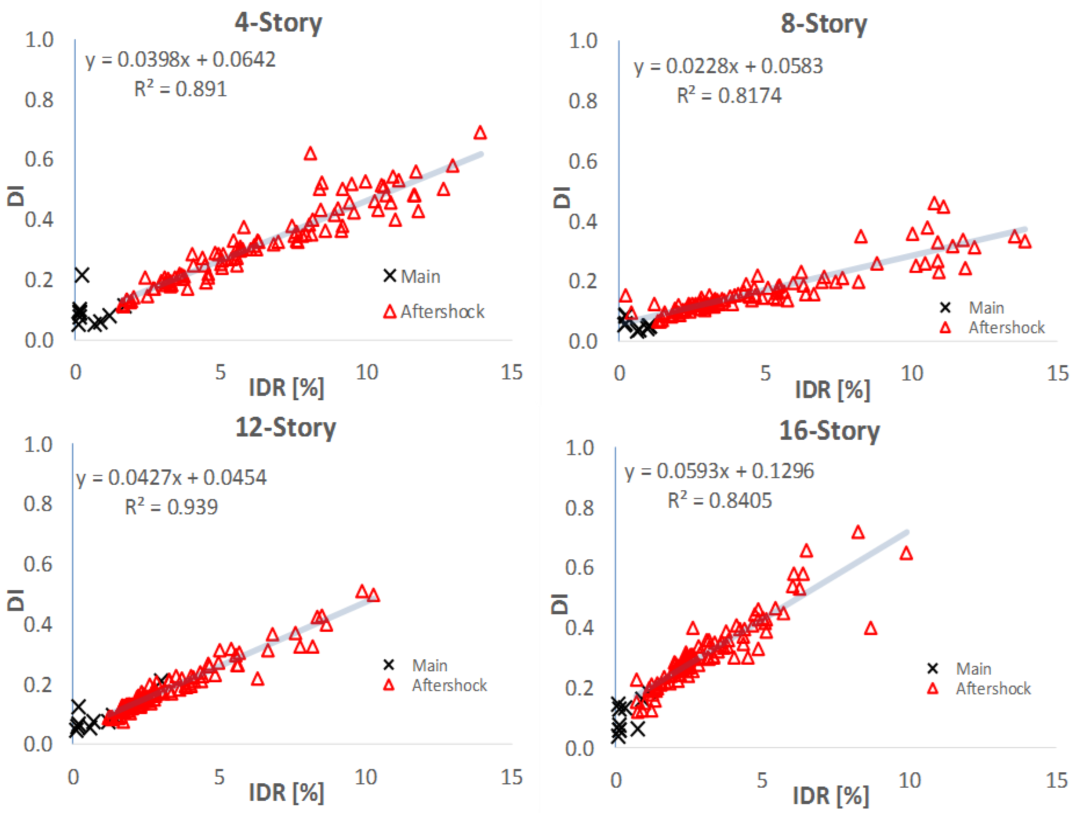

Fig. 10 Relationship between IDR and DI for mainshocks and major aftershocks

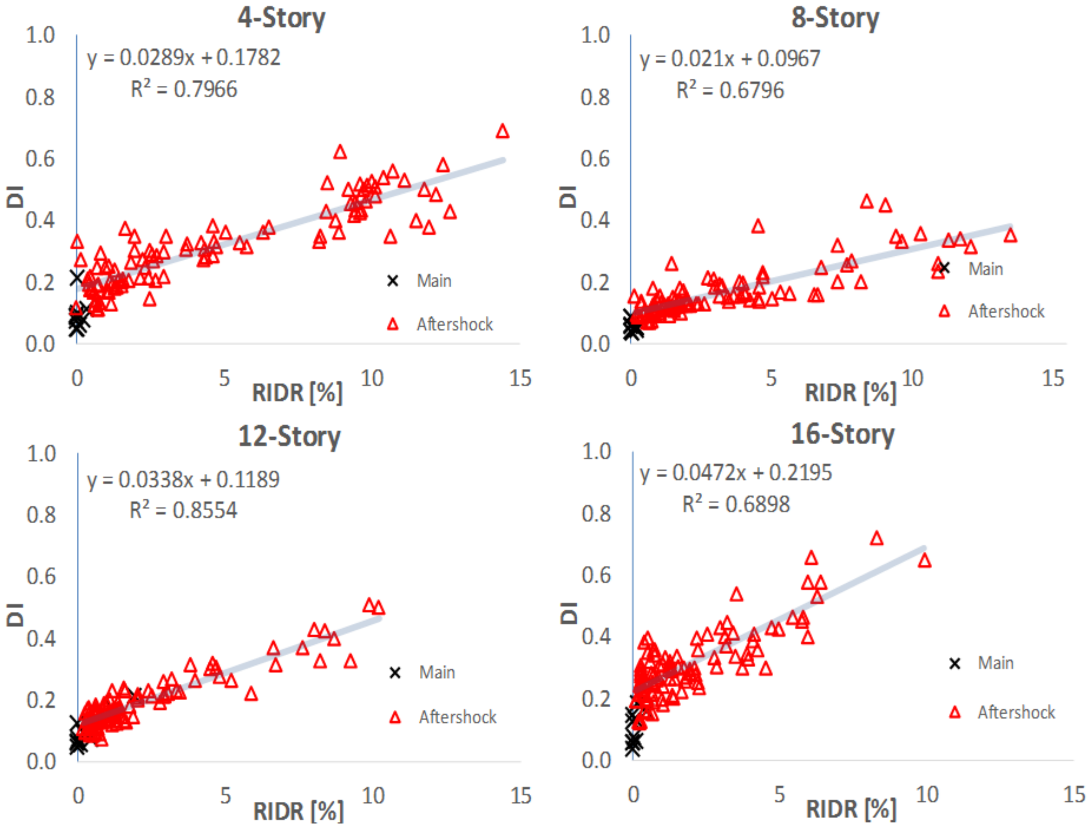

Fig. 11 Relationship between RIDR and damage index for mainshocks and main aftershocks

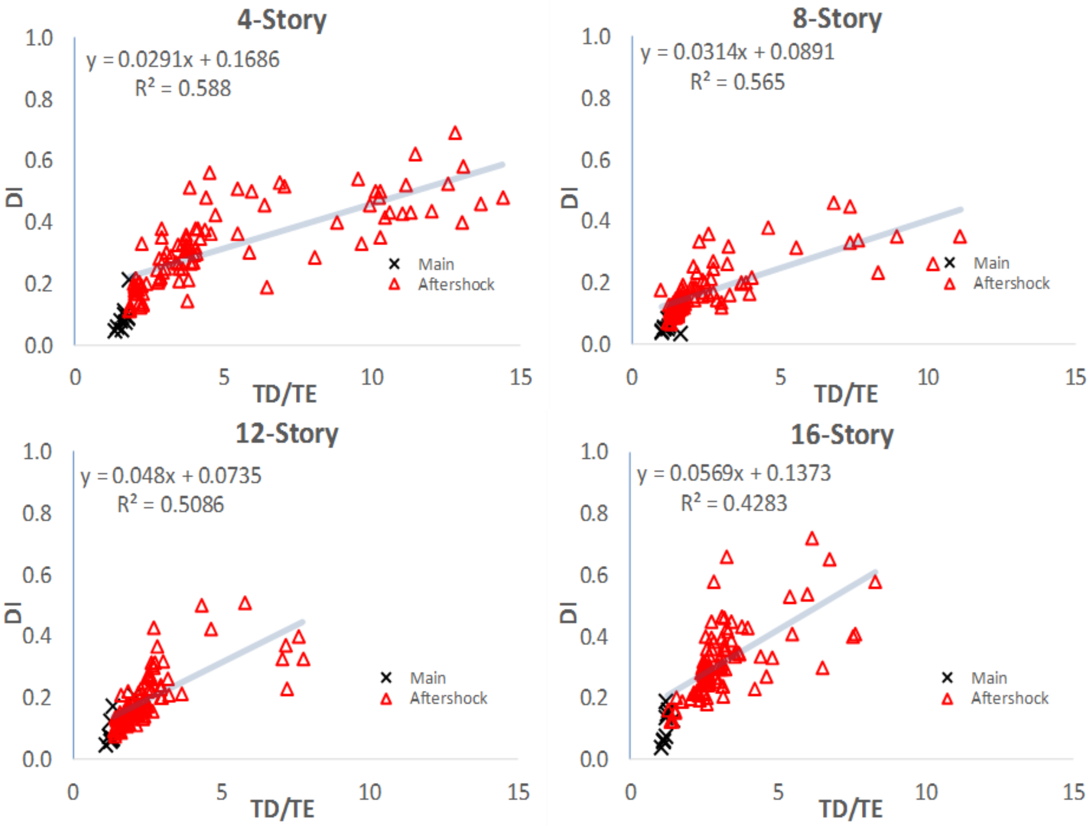

Fig. 12 DI vs TD/TE under FF-NF sequences

Table 6 Values of parameters a and b

Frame model	IDR			RIDR		
	a	*b*	R^2	*a*	*b*	R^2
4-story	0.0398	0.0642	0.89	0.0289	0.1782	0.80
8-story	0.0228	0.0583	0.82	0.0210	0.0967	0.68
12-story	0.0427	0.0454	0.94	0.0338	0.1189	0.85
16-story	0.0593	0.1296	0.84	0.0472	0.2195	0.69

5. Conclusions

The main objective of this study was to evaluate the seismic response of reinforced concrete frames subjected to far-field mainshock, near-fault aftershock sequences. The inter-story drift ratio, IDR, residual inter-story drift, RIDR, as well as the Park-Ang damage index DI, were considered as engineering demand parameters to study the influence of NF aftershocks on the relationships of the aforementioned engineering demands parameters for a family of RC frames designed with the current Iranian seismic code. The following conclusions are extracted from the results of this study

- Strong NF aftershocks can cause a significant increment in the structural damage of the case-study RC frames. The relationship between DI and IDR as well as RIDR appears to follow a linear trend once the RC frames are hit by the aftershocks.
- If the frame sustained a slight damage under the FF mainshock, it would be expected that NF aftershocks will have significant effects on the damaged frame. For example, the effect of aftershocks on the AVR.IDR parameter of damaged frames increased more than 4-fold.
- The shortest and tallest frames (4- and 16-story) showed larger increasing trends in the DI as a function of the increment of IDR and RIDR under the NF aftershocks.
- The IDR and DI were concentrated in the top stories of the shortest (4-story) frames and the lower stories of the tallest (16-story) frames. This appears to have caused the damaged 4- and 16-story frames to experience an increasing trend in their inelastic responses under NF aftershocks. However, the structural damage to the medium-height frames was distributed in all stories.
- Designers should consider the effect of strong NF aftershocks in their design approaches to decrease the expected damage.

Acknowledgments

This research was supported by the Kharazmi University Grant. While the first and third authors would like to thank the Kharazmi University in Iran, the second author would like thank Universidad Michoacana de San Nicolas de Hidalgo in Mexico.

References

Abdelnaby, A.E. and Elnashai, A.S. (2015), "Numerical modeling and analysis of RC frames subjected to multiple earthquakes", *Earthq. Struct.*, **9**(5), 957-981. http://dx.doi.org/10.12989/eas.2015.9.5.957

ACI 318 (2008), Building code requirements for structural concrete and commentary, American Concrete Institute; Farmington Hills, MI, USA.

Aghagholizadeh, M. and Massumi, A. (2016), "A new method to assess damage to RCMRFs from period elongation and Park-Ang damage index using IDA", *J. Adv. Struct. Eng.*, **8**(3), 243-252. https://doi.org/10.1007/s40091-016-0127-8.

Aki, K. (1984), "Asperities, barriers, characteristic earthquakes and strong motion prediction", *J. Geophys. Res. Solid Earth*, **89**(B7),5867-5872. https://doi.org/10.1029/JB089iB07p05867

Bazzurro, P., Cornell, C.A., Menun, C. and Motahari, M. (2004), "Guidelines for Seismic assessment of damaged buildings", *Proceedings of the 13th World Conference on Earthquake Engineering*, Vancouver, Canada, August.

Bradley, B.A. (2012), "Ground motions observed in the Darfield and Christchurch earthquakes and the importance of local site response effects", *New Zealand J. Geology Geophys.*, **55**(3), 279-286. https://doi.org/10.1080/00288306.2012.674049.

Cao, V.V., Ronagh, H.R., Ashraf, M. and Baji, H. (2014), "A new damage index for reinforced concrete structures", *Earthq. Struct.*, **6**(6), 581-609. http://dx.doi.org/10.12989/eas.2014.6.6.581

Chen, B. and Xu, Y. (2007), "A new damage index for detecting sudden change of structural stiffness", *Struct. Eng. Mech.*, **26**(3), 315-341. http://dx.doi.org/10.12989/sem.2007.26.3.315

Diaz-Martinez, G., Ruiz-García, J. and Terán-Gilmore, A. (2014). "Response of structures to seismic sequences corresponding to Mexican soft soils", *Earthq. Struct.*, **7**(6), 1241-1258. http://dx.doi.org/10.12989/eas.2014.7.6.1241

Eurocode 8 (2005), Design of structures for earthquake resistance, European Committee for Standardization, United Kingdom.

Faisal, A., Majid, T.A. and Hatzigeorgiou, G.D. (2013), "Investigation of story ductility demands of inelastic concrete frames subjected to repeated earthquakes", *Soil Dynam. Earthq. Eng.*, **44**, 42-53. https://doi.org/10.1016/j.soildyn.2012.08.012

Ghobarah, A. (2004), "On drift limits associated with different damage levels. in Performance-Based Seismic Design Concepts and Implementation", *Proceedings of the International Workshop*, Bled, Slovenia.

Habibi, A., Vahed, M. and Asadi, K. (2018). "Evaluation of Seismic performance of RC setback frames", *Struct. Eng. Mech.*, **66**(5), 609-619. http://dx.doi.org/10.12989/sem.2018.66.5.609

Hatzigeorgiou, G.D. and Beskos, D.E. (2009), "Inelastic displacement ratios for SDOF structures subjected to repeated earthquakes", *Eng. Struct.*, **31**(11), 2744-2755. https://doi.org/10.1016/j.engstruct.2009.07.002

Hosseini, S.A. (2016), "Seismic behavior of RC structures under far-field and near-fault mainshock–aftershock seismic sequences", M.Sc. Dissertation, Kharazmi University, Tehran, Iran.

Hosseinpour, F. and Abdelnaby, A. (2017), "Effect of different aspects of multiple earthquakes on the nonlinear behavior of RC structures", *Soil Dynam. Earthq. Eng.*, **92**, 706-725. https://doi.org/10.1016/j.soildyn.2016.11.006

Kang, J. W. and Lee, J. (2016). "A new damage index for seismic fragility analysis of reinforced concrete columns", *Struct. Eng. Mech.*, **60**(5), 875-890. http://dx.doi.org/10.12989/sem.2016.60.5.875

Kim, T. and Kim, J. (2007), "Seismic performance evaluation of a RC special moment frame", *Struct. Eng. Mech.*, **27**(6), 671-682. http://dx.doi.org/10.12989/sem.2007.27.6.671

Kostinakis, K. and Morfidis, K. (2017), "The impact of successive earthquakes on the seismic damage of multistorey 3D R/C buildings", *Earthq. Struct.*, **12**(1), 1-12. http://dx.doi.org/10.12989/eas.2017.12.1.001

Liu, Y., Yu, X.-H. Lu, D.-G. and Ma, F.-Z. (2018), "Impact of initial damage path and spectral shape on aftershock collapse fragility of RC frames", *Earthq. Struct.*, **15**(5), 529-540. http://dx.doi.org/10.12989/eas.2018.15.5.529

Mahin, S.A. (1985), "Effects of duration and aftershocks on inelastic design earthquakes", *Proceedings of the 7th World Conference on Earthquake Engineering*, Istanbul, Turkey.

Maniyar, M., Khare, R. and Dhakal, R. (2009), "Probabilistic seismic performance evaluation of non-seismic RC frame buildings", *Struct. Eng. Mech.*, **33**(6), 725-745. http://dx.doi.org/10.12989/sem.2009.33.6.72

Massumi, A. and Moshtagh, E. (2013), "A new damage index for RC buildings based on variations of nonlinear fundamental period", *Struct. Design Tall Special Build.*, **22**(1), 50-61. https://doi.org/10.1002/tal.656

Massumi, A., Sadeghi, K. and Moshtagh, E. (2018), "Effects of deviation in materials' strengths on the lateral strength and damage of RC frames", *Struct. Eng. Mech.*, **68**(3), 289-297. http://dx.doi.org/10.12989/sem.2018.68.3.289

Mirtaheri, M., Amini M. and Rad, M.D. (2017), "The effect of mainshock-aftershock on the residual displacement of buildings equipped with cylindrical frictional damper", *Earthq. Struct.*, **12**(5), 515-527. http://dx.doi.org/10.12989/eas.2017.12.5.515

Moustafa, A. and Takewaki, I. (2010), "Characterization and modeling of near-fault pulse-like strong ground motion via damage-based critical excitation method", *Struct. Eng. Mech.*, **34**(6), 755-788. http://dx.doi.org/10.12989/sem.2010.34.6.755

Moustafa, A. and Takewaki, I. (2012), "Characterization of earthquake ground motion of multiple sequences", *Earthq. Struct.*, **3**(5), 629-647. http://dx.doi.org/10.12989/eas.2012.3.5.629

Naderpour, H. and Vakili, K. (2019), "Safety assessment of dual shear wall-frame structures subject to Mainshock-Aftershock sequence in terms of fragility and vulnerability curves", *Earthq. Struct.*, **16**(4), 425-436. http://dx.doi.org/10.12989/eas.2019.16.4.425

Park, Y.-J. and Ang, A.H.-S. (1985a), "Mechanistic seismic damage model for reinforced concrete", *J. Struct. Eng.*, **111**(4), 722-739. https://doi.org/10.1061/(ASCE)0733-9445(1985)111:4(722)

Park, Y.-J., Ang, A.H.-S. and Wen, Y.K. (1985b), "Seismic damage analysis of reinforced concrete buildings", *J. Struct. Eng.*, **111**(4), 740-757. https://doi.org/10.1061/(ASCE)0733-9445(1985)111:4(740)

Potter, S.H., Becker, J.S., Johnston, D.M. and Rossiter, K.P. (2015), "An overview of the impacts of the 2010-2011 Canterbury earthquakes", *J.Disaster Risk Reduction*, **14**(1), 6-14. https://doi.org/10.1016/j.ijdrr.2015.01.014

Reinhorn, A., Roh, Sivaselvan, H. M., Kunnath, S.K., Valles, R.E., Madan, A., Li, Lobo, C. R. and Park, Y. (2009), *IDARC 2D version 7.0*, A program for the inelastic damage analysis of buildings, Buffalo, New York, USA.

Ruff, L. and Kanamori, H. (1983), "Seismic coupling and uncoupling at subduction zones", *Tectonophysics*, **99**(2-4), 99-117. https://doi.org/10.1016/0040-1951(83)90097-5

Ruiz-García, J. and Negrete-Manriquez, J.C. (2011), "Evaluation of drift demands in existing steel frames under as-recorded far-field and near-fault mainshock–aftershock seismic sequences", *Eng. Struct.*, **33**(2), 621-634. https://doi.org/10.1016/j.engstruct.2010.11.021

Ruiz-García, J. and Aguilar, J.D. (2015), "Aftershock seismic assessment taking into account postmainshock residual drifts", *Earthq. Eng. Struct. Dynam.*, **44**(9), 1391-1407. https://doi.org/10.1002/eqe.2523

Ruiz-García, J. (2012), "Mainshock-aftershock ground motion features and their influence in building's seismic response", *J. Earthq. Eng.*, **16**(5), 719-737. https://doi.org/10.1080/13632469.2012.663154

Ruiz-García, J., Marín, M.V. and Terán-Gilmore, A. (2014), "Effect of seismic sequences in reinforced concrete frame buildings located in soft-soil sites", *Soil Dynam. Earthq. Eng.*, **63**, 56-68. https://doi.org/10.1016/j.soildyn.2014.03.008

Ruiz-García, J., Yaghmaei-Sabegh, S., Bojórquez, E. (2018), "Three-dimensional response of steel moment-resisting buildings under seismic sequences", *Eng. Struct.*, **175**, 399-414. https://doi.org/10.1016/j.engstruct.2018.08.050

Sakka, Z.I., Asskkaf, I.A., and Qazweeni, J.S. (2018). "Reliability-based assessment of damaged concrete buildings", *Struct. Eng. Mech.*, **65**(6), 751-760. http://dx.doi.org/10.12989/sem.2018.65.6.751

Shcherbakov, R., Yakovlev, G., Turcotte, D.L., and Rundle, J.B. (2005) "Model for the distribution of aftershock interoccurrence times", *Phys. Review Lett.*, **95**(21), https://doi.org/10.1103/PhysRevLett.95.218501

Shokrabadi, M. and H. V. Burton (2018), "Risk-based assessment of aftershock and mainshock-aftershock seismic performance of reinforced concrete frames", *Struct. Safety,* **73**, 64-74. https://doi.org/10.1016/j.strusafe.2018.03.003

Standard No. 2800-05, Iranian Code of Practice for Seismic Resistant Design of Buildings, 3rd Edition, Building and Housing Research Center, Tehran, Iran.

Yaghmaei-Sabegh, S. and Ruiz-García, J. (2016), "Nonlinear response analysis of SDOF systems subjected to doublet earthquake ground motions: A case study on 2012 Varzaghan–Ahar events", *Eng. Struct.*, **110**, 281-292. https://doi.org/10.1016/j.engstruct.2015.11.044

Zhai, C.H., Wen, W.P., Chen, A.Q., Li, Sh., and Xie, L.L. (2013), "Damage spectra for the mainshock–aftershock sequence-type ground motions", *Soil Dynam. Earthq. Eng.*, **45**, 1-12. https://doi.org/10.1016/j.soildyn.2012.10.001

Zhai, C.H., Wen, W.P., Li, Sh., and Xie, L.L. (2014), "The damage investigation of inelastic SDOF structure under the mainshock-aftershock sequence-type ground motions", *Soil Dynam. Earthq. Eng.*, **59**, 30-41. https://doi.org/10.1016/j.soildyn.2014.01.003

Zhai, C.H., Wen, W.P., Li, Sh., and Xie, L.L. (2015), "The ductility-based strength reduction factor for the mainshock-aftershock sequence-type ground motions", *Bullet. Earthq. Eng.*, **13**(10), 2893-2914. https://doi.org/10.1007/s10518-015-9744-z

Zhang, Y., Chen, J., and Sun, C. (2017), "Damage-based strength reduction factor for nonlinear structures subjected to sequence-type ground motions", *Soil Dynam. Earthq. Eng.*, **92**, 298-311. https://doi.org/10.1016/j.soildyn.2016.10.002

CC